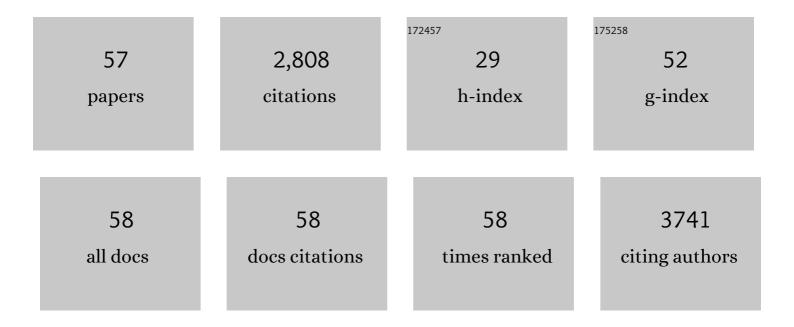
George E Hilley

List of Publications by Year in descending order

Source: https://exaly.com/author-pdf/3239008/publications.pdf Version: 2024-02-01



#	Article	IF	CITATIONS
1	Dynamics of Slow-Moving Landslides from Permanent Scatterer Analysis. Science, 2004, 304, 1952-1955.	12.6	409
2	Resolving vertical tectonics in the San Francisco Bay Area from permanent scatterer InSAR and GPS analysis. Geology, 2006, 34, 221.	4.4	175
3	Major ion chemistry of the Yarlung Tsangpo–Brahmaputra river: Chemical weathering, erosion, and CO2 consumption in the southern Tibetan plateau and eastern syntaxis of the Himalaya. Geochimica Et Cosmochimica Acta, 2007, 71, 2907-2935.	3.9	161
4	Uplift, Erosion, and Phosphorus Limitation in Terrestrial Ecosystems. Ecosystems, 2007, 10, 159-171.	3.4	161
5	Chemical weathering, mass loss, and dust inputs across a climate by time matrix in the Hawaiian Islands. Earth and Planetary Science Letters, 2007, 258, 414-427.	4.4	122
6	Constraints on the late Quaternary glaciations in Tibet from cosmogenic exposure ages of moraine surfaces. Quaternary Science Reviews, 2011, 30, 528-554.	3.0	109
7	Geomorphic response to uplift along the Dragon's Back pressure ridge, Carrizo Plain, California. Geology, 2008, 36, 367.	4.4	106
8	Processes of oscillatory basin filling and excavation in a tectonically active orogen: Quebrada del Toro Basin, NW Argentina. Bulletin of the Geological Society of America, 2005, 117, 887.	3.3	101
9	Terrestrial source to deep-sea sink sediment budgets at high and low sea levels: Insights from tectonically active Southern California. Geology, 2011, 39, 619-622.	4.4	101
10	A framework for predicting global silicate weathering and CO ₂ drawdown rates over geologic time-scales. Proceedings of the National Academy of Sciences of the United States of America, 2008, 105, 16855-16859.	7.1	95
11	Climatic control of denudation in the deglaciated landscape of the Washington Cascades. Nature Geoscience, 2011, 4, 469-473.	12.9	95
12	Rate-weakening friction characterizes both slow sliding and catastrophic failure of landslides. Proceedings of the National Academy of Sciences of the United States of America, 2016, 113, 10281-10286.	7.1	80
13	Multitemporal ALSM change detection, sediment delivery, and process mapping at an active earthflow. Earth Surface Processes and Landforms, 2012, 37, 262-272.	2.5	76
14	Average Pleistocene Climatic Patterns in the Southern Central Andes: Controls on Mountain Glaciation and Paleoclimate Implications. Journal of Geology, 2002, 110, 211-226.	1.4	69
15	Hillslopes Record the Growth and Decay of Landscapes. Science, 2013, 341, 868-871.	12.6	62
16	Benchmarking analogue models of brittle thrust wedges. Journal of Structural Geology, 2016, 92, 116-139.	2.3	58
17	Differential structural and geomorphic mountain-front evolution in an active continental collision zone: The northwest Pamir, southern Kyrgyzstan. Bulletin of the Geological Society of America, 2003, 115, 166-181.	3.3	57
18	Linking chronosequences with the rest of the world: predicting soil phosphorus content in denuding landscapes. Biogeochemistry, 2011, 102, 153-166.	3.5	56

GEORGE E HILLEY

#	Article	IF	CITATIONS
19	The chemical, mechanical, and hydrological evolution of weathering granitoid. Journal of Geophysical Research F: Earth Surface, 2016, 121, 1410-1435.	2.8	49
20	Influence of attenuated lithosphere and sediment loading on flexure of the deep-water Magallanes retroarc foreland basin, Southern Andes. Tectonics, 2014, 33, 2505-2525.	2.8	47
21	Earthquake-cycle deformation and fault slip rates in northern Tibet. Geology, 2009, 37, 31-34.	4.4	45
22	Early evolution of an extensional monocline by a propagating normal fault: 3D analysis from combined field study and numerical modeling. Journal of Structural Geology, 2002, 24, 651-669.	2.3	41
23	Depth and character of rock weathering across a basalticâ€hosted climosequence on Hawaiâ€~i. Earth Surface Processes and Landforms, 2014, 39, 381-398.	2.5	41
24	The relationship between tectonic uplift and chemical weathering rates in the Washington Cascades: Field measurements and model predictions. Numerische Mathematik, 2007, 307, 1041-1063.	1.4	38
25	Lithologic control on the form of soil-mantled hillslopes. Geology, 2015, 43, 83-86.	4.4	37
26	Morphologic dating of fault scarps using airborne laser swath mapping (ALSM) data. Geophysical Research Letters, 2010, 37, .	4.0	35
27	Earth's topographic relief potentially limited by an upper bound on channel steepness. Nature Geoscience, 2019, 12, 828-832.	12.9	35
28	A Test of Initiation of Submarine Leveed Channels by Deposition Alone. Journal of Sedimentary Research, 2010, 80, 710-727.	1.6	34
29	Large uncertainty in permafrost carbon stocks due to hillslope soil deposits. Geophysical Research Letters, 2017, 44, 6134-6144.	4.0	31
30	Erosion, Geological History, and Indigenous Agriculture: A Tale of Two Valleys. Ecosystems, 2010, 13, 782-793.	3.4	25
31	Symmetry, randomness, and process in the structure of branched channel networks. Geophysical Research Letters, 2014, 41, 3485-3493.	4.0	24
32	Fault zone structure from topography: Signatures of en echelon fault slip at Mustang Ridge on the San Andreas Fault, Monterey County, California. Tectonics, 2010, 29, n/a-n/a.	2.8	22
33	The sensitivity of turbidity currents to mass and momentum exchanges between these underflows and their surroundings. Journal of Geophysical Research, 2012, 117, .	3.3	22
34	Restraining bend tectonics in the Santa Cruz Mountains, California, imaged using 10Be concentrations in river sands. Geology, 2013, 41, 843-846.	4.4	22
35	Detection of CO2 leakage by eddy covariance during the ZERT project's CO2 release experiments. Energy Procedia, 2009, 1, 2301-2306.	1.8	19
36	Eddy covariance imaging of diffuse volcanic CO2 emissions at Mammoth Mountain, CA, USA. Bulletin of Volcanology, 2012, 74, 135-141.	3.0	19

GEORGE E HILLEY

#	Article	IF	CITATIONS
37	Deducing Paleoearthquake Timing and Recurrence from Paleoseismic Data, Part I: Evaluation of New Bayesian Markov-Chain Monte Carlo Simulation Methods Applied to Excavations with Continuous Peat Growth. Bulletin of the Seismological Society of America, 2008, 98, 383-406.	2.3	17
38	Interaction between normal faults and fractures and fault scarp morphology. Geophysical Research Letters, 2001, 28, 3777-3780.	4.0	14
39	Eddy covariance network design for mapping and quantification of surface CO2 leakage fluxes. International Journal of Greenhouse Gas Control, 2012, 7, 137-144.	4.6	10
40	Inferring Segment Strength Contrasts and Boundaries along Low-Friction Faults Using Surface Offset Data, with an Example from the Cholame-Carrizo Segment Boundary along the San Andreas Fault, Southern California. Bulletin of the Seismological Society of America, 2001, 91, 427-440.	2.3	8
41	Erosional control of the kinematics of the Aconcagua fold-and-thrust belt from numerical simulations and physical experiments. Geology, 2011, 39, 439-442.	4.4	8
42	Weak bedrock allows north-south elongation of channels in semi-arid landscapes. Earth and Planetary Science Letters, 2017, 478, 150-158.	4.4	8
43	Turbidity Current Dynamics: 2. Simulating Flow Evolution Toward Equilibrium in Idealized Channels. Journal of Geophysical Research F: Earth Surface, 2018, 123, 520-534.	2.8	8
44	Regionalâ€Scale Detection of Fault Scarps and Other Tectonic Landforms: Examples From Northern California. Journal of Geophysical Research: Solid Earth, 2019, 124, 1016-1035.	3.4	8
45	Deducing Paleoearthquake Timing and Recurrence from Paleoseismic Data, Part II: Analysis of Paleoseismic Excavation Data and Earthquake Behavior along the Central and Southern San Andreas Fault. Bulletin of the Seismological Society of America, 2008, 98, 407-439.	2.3	7
46	The Pamir Frontal Thrust Fault: Holocene Fullâ€Segment Ruptures and Implications for Complex Segment Interactions in a Continental Collision Zone. Journal of Geophysical Research: Solid Earth, 2021, 126, e2021JB022405.	3.4	6
47	Adding a community partner to service learning may elevate learning but not necessarily service. International Journal of Disaster Risk Reduction, 2018, 28, 80-87.	3.9	5
48	Are submarine and subaerial drainages morphologically distinct?. Geology, 2019, 47, 1093-1097.	4.4	5
49	Bridging earthquakes and mountain building in the Santa Cruz Mountains, CA. Science Advances, 2022, 8, eabi6031.	10.3	5
50	Turbidity Current Dynamics: 1. Model Formulation and Identification of Flow Equilibrium Conditions Resulting From Flow Stripping and Overspill. Journal of Geophysical Research F: Earth Surface, 2018, 123, 501-519.	2.8	4
51	Millennial-scale denudation rates of the Santa Lucia Mountains, California: Implications for landscape evolution in steep, high-relief, coastal mountain ranges. Bulletin of the Geological Society of America, 2018, 130, 1809-1824.	3.3	4
52	A Curvatureâ€Based Method for Measuring Valley Width Applied to Glacial and Fluvial Landscapes. Journal of Geophysical Research F: Earth Surface, 2020, 125, e2020JF005605.	2.8	4
53	What Do Kinematic Models Imply About the Constitutive Properties of Rocks Deformed in Flatâ€Rampâ€Flat Folds?. Geophysical Research Letters, 2017, 44, 9581-9588.	4.0	3
54	Scarplet: A Python package for topographic template matching and diffusion dating. Journal of Open Source Software, 2018, 3, 1066.	4.6	3

#	Article	IF	CITATIONS
55	Encouraging Earthquake-Resistant Construction: A Randomized Controlled Trial in Nepal. Earthquake Spectra, 2016, 32, 1975-1988.	3.1	2
56	pymccrgb: Color- and curvature-based classification of multispectral point clouds in Python. Journal of Open Source Software, 2019, 4, 1777.	4.6	0
57	Seasonal and Multiyear Changes in CO ₂ Degassing at Mammoth Mountain Explained by Solidâ€Earthâ€Driven Fault Valving. Geophysical Research Letters, 2022, 49, .	4.0	Ο